Spectrum of Engineering Sciences
ISSN (e) 3007-3138 (p) 3007-312X Volume 4, Issue 2, 2026

DEEP LEARNING-ENHANCED DETECTION OF PATHOLOGICAL MYOPIA VIA MULTI-FEATURE FUSION AND PRECISE RETINAL SEGMENTATION

Laiba Gul[1], Sabahat Ijaz[2], Noormah Omar Khan[3], Sehrish Taimoor[4], Muhammad Uzair[*5]

[1]*Department of Computer Science and Engineering, Chalmers University of Technology and University of Gothenburg, Gothenburg, Sweden*
[2,3,*5]*Department of Computer Science, National University of Computer and Emerging Sciences, Islamabad, Pakistan*
[4]*Department of Biological & Environmental Sciences, University of Gothenburg, Gothenburg, Sweden*

[1]laibalg6117@gmail.com, [2]sabahat26@gmail.com, [3]nooraekh@gmail.com,
[4]sehrishzeeshan4@gmail.com, [*5]muhammaduzair98@gmail.com

DOI: https://doi.org/10.5281/zenodo.18654329

Keywords
Pathological Myopia, Deep Learning Segmentation, U-Net Architecture, Multi-Feature Fusion, Support Vector Machine, Fundus Image Analysis

Article History
Received: 15 December 2025
Accepted: 30 January 2026
Published: 16 February 2026

Corresponding Author: *
Muhammad Uzair

Abstract
Pathological Myopia (PM) is a major cause of permanent blindness in the world, but it is difficult to detect during its early development as there is a complex and diverse manifestation of retinal lesions. This research provides an automated diagnostic scheme, which makes use of a multi-feature fusion model to categorize fundus images into normal, highly myopic and pathologically myopic groups. The system identifies five clinical biomarkers, including Fuchs Spots, Lattice Degeneration, Posterior Staphyloma, Tigroid Fundus, and Peripapillary Atrophy (PPA). To combat the problem of inaccurate localization of optic disk, one of the main errors in the previous PPA-based models, this work uses a U-Net deep learning structure to perform high-quality segmentation. A combination of the Gray Level Co-occurrence Matrix (GLCM) which was used to analyze texture and Oriented FAST and Rotated BRIEF which was used to detect localized lesions were used to extract features. These multi-dimensional characteristics were fed to Support Vector Machine (SVM) classifier. The combined model was tested on a test set of 400 fundus images and the individual model showed a diagnostic accuracy of about 90.15. The 10-fold cross-validation revealed that the system is robust, as the U-Net-enhanced PPA feature has the highest score of 92.27 in the validation. These results indicate that a multi-feature analysis is a useful way of overcoming the drawbacks of mono-marker detection and can be viewed as a reliable and objective tool to detect myopic blindness and apply preventive strategies in the course of early clinical intervention.

INTRODUCTION

Myopia, commonly called near sightedness, is the condition of the vision in which the lens of the eye focuses the images in front of the retina instead of directly on it, making objects appearing in the distance blurred. Pathological Myopia (PM) is a serious type of this HCC with a high refractive error of more than -6 Diopters. This great degree of myopia causes the eyeball to elongate (substantially stretch and thin out the retina and sclera). As shown in Figure 1 these

physical changes lead to degenerative changes to the back of the eye which can lead to permanent vision loss and predispose to other serious eye diseases like Glaucoma [1].

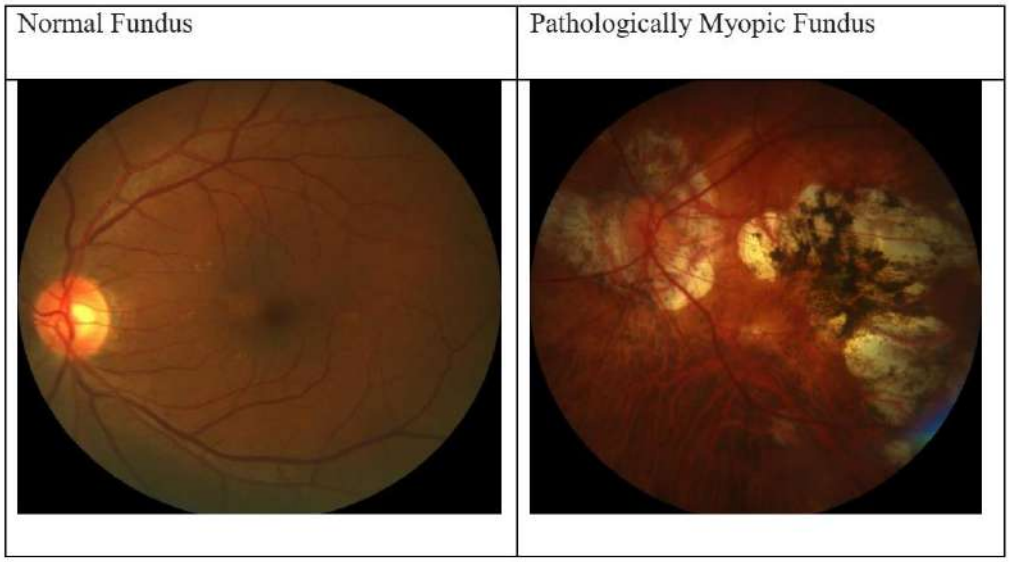

Figure 1: Comparison of a Normal Fundus Vs. A Pathologically Myopic Fundus

The worldwide effect of this condition is reaching critical levels. According to reports from the World Health Organization (WHO), the number of people suffering from myopia is set to triple in the next three decades to reach from 300 million to around 925 million cases. Projections show that by 2050, high myopia will affect around 10% of the world's population. Given these alarming statistics, there is a "dire need" for objective and automated systems which can detect and monitor the progress of Pathological Myopia in order to facilitate clinical intervention at an early stage [2].

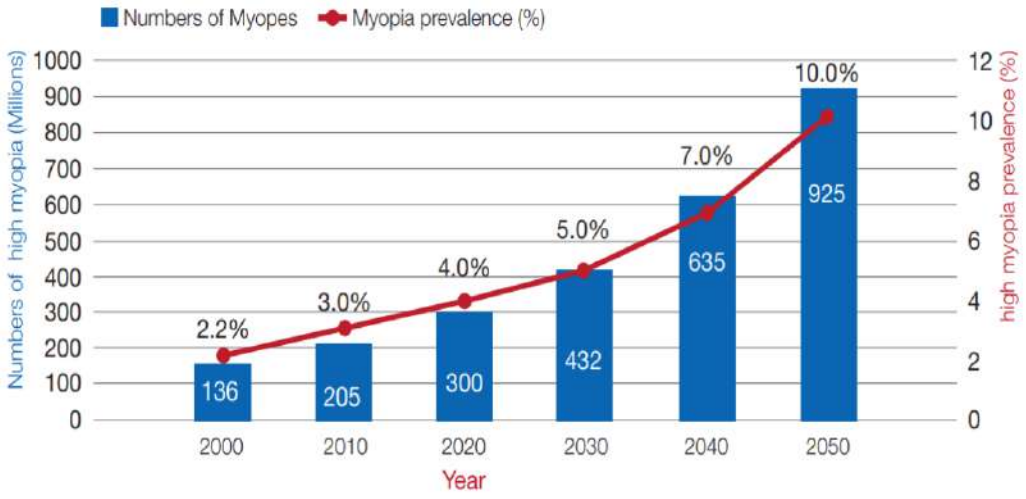

Figure 2: Global prevalence projections of high myopia (2000–2050) based on WHO data [3]

Current diagnostic workflows are highly reliant on the manual testing of visual acuity, which poses a number of challenges in operation. These methods are time-consuming, labor-intensive, and

subconsciously biased by nature because they rely on a patient's own evaluation of his or her vision, which can produce inconsistent results, particularly in younger patients. Furthermore, most current computational methods for automated detection are based mostly on one particular symptom: Peripapillary Atrophy (PPA). However, these systems are prone to fail if the Optic Disk (OD) is not perfectly centered in the fundus image and thus accurate PPA estimations are not present. This research overcomes these limitations by proposing a strong and multi-feature detection framework. In addition to Peripapillary Atrophy, the proposed system extracts and analyzes a rich set of pathological markers such as Posterior Staphyloma, Fuchs spots, Tigroid Fundus and Lattice Degeneration. By combining these diverse clinical symptoms and by applying a U-Net architecture for accurate segmentation of the Optic Disk, the current work could enhance diagnosis accuracy of the clinical symptoms and reduce the time and cost of detecting Pathological Myopia[4][5].

1. Literature Review

The automated detection of Pathological Myopia (PM) has mainly been concentrated into the identification of Peripapillary Atrophy (PPA), a well-known clinical sign of the disease that is characterized by the recession of the retinal pigment epithelium around the optic nerve head [6]. Early attempts at computation made use of histogram-based methods for feature extraction, based on the fact that the optic nerve head normally has the highest intensity in the red channel of eviscerated image. These methods were often supplemented by texture analysis to measure the rate of the atrophy [7]. For example, researchers have used variational level set methods to delineate the internal and external regions of the optic disk, and then have applied color space transformations to verify the presence of PPA [4].

Despite these advancements, in the literature there is a major shortfall found in Optic Disk (OD) localization in terms of robustness. Many conventional systems work on the presumption that the optic disk is centrally located in the fundus image, and therefore, if the optic disk is out of center, or the image is poor, these systems tend to make erroneous estimations of the PPA [8]. To enhance the diagnostic accuracy, more recent studies have been carried out on multi-feature selection methods, Minimum Redundancy-Maximal Relevancy (mRMR) helps in identifying a subset of features maximally relevant to the pathology and with the least redundancy among the data [9].

Beyond just measures of intensity, the combination of low-level image features has become one of the major themes of research in PM. Texture-based features are often applied to image contents to describe the coarseness and regularity of images, which are very helpful cases when the standard color features do not provide enough information for classifying the images [10]. Additionally, shape-based and geometric features, like points, lines and ridges, are important to analyzing the physical structure of the eye and increasing object recognition accuracy. Some frameworks have also made the Bag-of-Features (BoF) model, which describes global properties of the image by counting the occurrences of local feature descriptors (i.e. keeping invariance to rotation and intensity shifts) [11].

In recent times, there is a movement towards deep learning architectures and more complete symptom-based detection. While the initial studies were almost exclusively in the area of PPA, recent studies have highlighted the need to identify other types of pathological features such as Fuchs' spots, Tigroid Fundus and Posterior Staphyloma. The fact that the transition from traditional interest point detectors such as Harris or Hessian Laplacians to deep learning models such as U-Net enables more precise localization of the Optic Disk in even complex and non-centered images has helped provide more stable basis for subsequent extraction of pathological features [12]. Table 1 shows the summary of the related work.

Table 1: Summary of Related Work

Category	Specific Techniques	Key Function/Methodology	Limitations/Findings
Primary Marker Detection	Peripapillary Atrophy (PPA)	Segmentation of myopic atrophy using multi-center benchmarks [13].	Traditional PPA markers are now often integrated into broader myopic maculopathy scales.
Feature Extraction	Deep Texture Analysis	Utilization of CNN-based texture descriptors for identifying Tigroid Fundus [14].	Modern descriptors are more resilient to lighting variations than manual GLCM.
Geometric Analysis	Structural/Shape Features	Analysis of eyeball elongation and staphyloma via morphological modeling [17].	Essential for distinguishing High Myopia from Pathological Myopia.
Representation Models	Vision Transformers (ViT)	Global feature representation using self-attention mechanisms [15].	Captures long-range dependencies across the retina better than local BoF models.
Optimization	Multi-Task Learning	Simultaneous optimization of detection and segmentation tasks [14].	Reduces the need for manual feature selection (mRMR) by learning relevant features end-to-end.
Segmentation	Robust OD Localization	Deep learning frameworks for OD/Cup segmentation under challenging conditions [13], [16].	Advanced models now handle non-centered and low-quality clinical images effectively.
Proposed Work (This Research)	**U-Net Segmentation & Multi-Symptom Fusion**	**Deep learning-based OD localization combined with extraction of five distinct features (PPA, Staphyloma, Tigroid Fundus, Fuchs' Spots, Lattice Degeneration).**	**Overcomes OD localization failures; provides a holistic diagnosis by analyzing multiple pathologies; achieves high accuracy (~90%) across diverse image types.**

3. Methodology

The pipeline of the proposed system comprises a series of steps, whereby raw data can be first processed into deep learning that will subsequently be used to segment the data followed by multi-symptom feature extraction and lastly, automated classification. The flow diagram is a logical flow that transforms the raw retinal information into a clinical diagnosis. It starts by acquiring 400 fundus images which are prepared by Pre-processing (Green Channel conversion and CLAHE) to make maximum contrast of the features. The U-Net Segmentation block is the essence of the spatial analysis that separates the Optic Disk as the major Area of Interest. This is then succeeded by a Parallel Feature Extraction phase in which five separate markers of pathology (PPA, Tigroid Fundus, Fuch Spots etc.) are measured. Lastly, these attributes are combined and run through an SVM Classifier with 10-fold cross-validation to generate a conclusive diagnostic result with 90 percent accuracy.

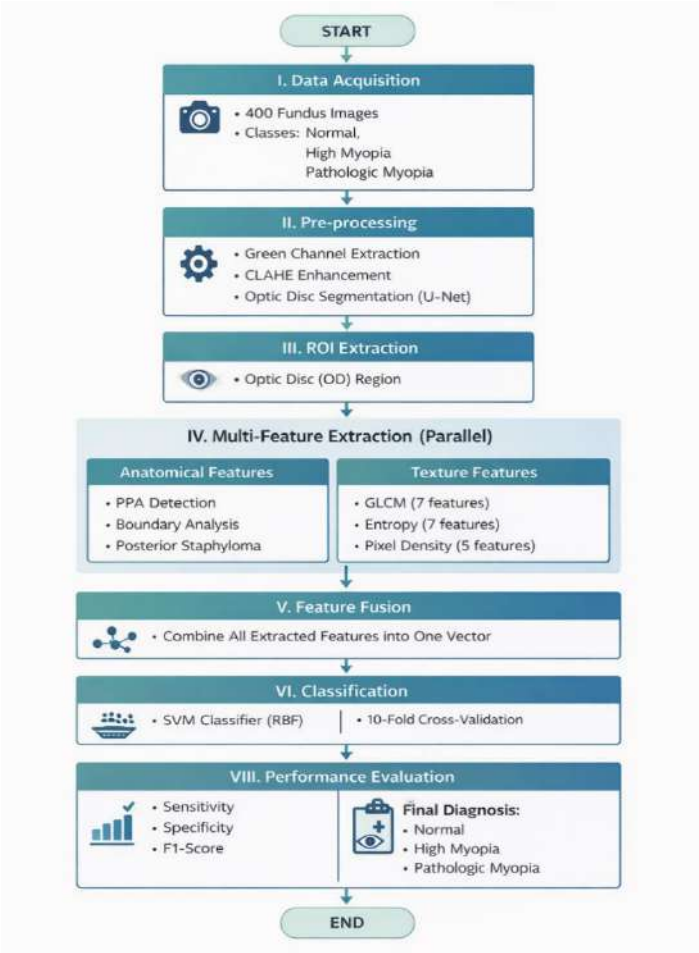

Figure 3: Flowchart of the proposed methodology

3.1 Acquisition, Preprocessing and ROI Extraction

Here a large dataset of 400 fundus images are utilized, which are classified as either Normal, Highly Myopic, and Pathological Myopia (PM). A preprocessing stage is adopted to standardize the input in order to prepare the images to be extracted. This is done by transforming images to particular channels of color i.e. the green channel; it gives the best contrast to the retinal structures. This is then followed by Contrast Limited Adaptive Histogram Equalization (CLAHE) that helps in making visible subtle pathological properties that include thinning retinal layers, atrophic patches and makes sure that the later extraction algorithms are working on high-quality input data.

3.1.1 Posterior Staphyloma:

The selective process of ROI extraction based on the green channel of the fundus image is isolated and Contrast Limited Adaptive Histogram Equalization (CLAHE) is applied in order to enhance the edges of the possible posterior staphyloma. Binary threshold in terms of characteristic color properties is then used to divide the region. To classify the data, two major characteristics are obtained the entropy of the area and the number of pixels (area). The number of extra pixels in these segments and their level of entropy are the main factors showing the indication of pathological myopia. The fundus image along with the flowchart is shown in figure 4.

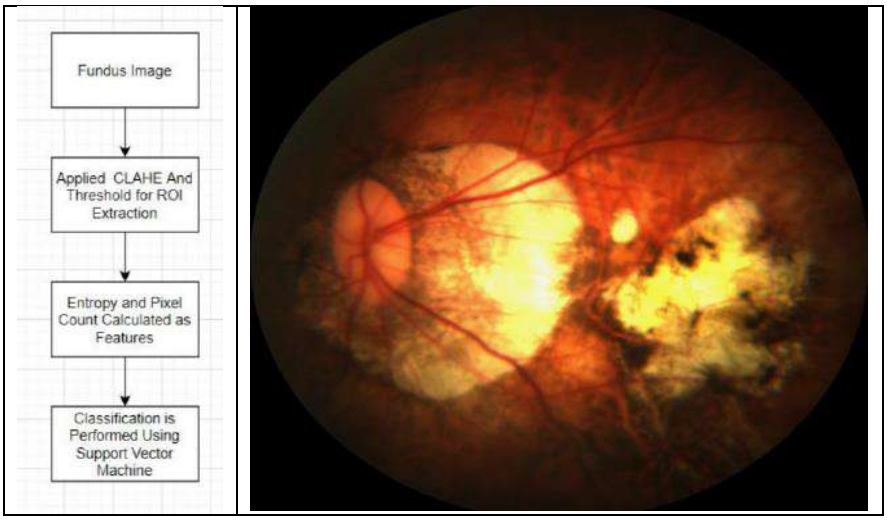

Figure 4: Flowchart and Image for Posterior Staphyloma Feature Extraction

3.1.2 Tigroid Fundus:

In order to isolate the dark and striped patterns of a Fundus that is tigroid in nature, the system uses a TOZERO_INV threshold of the grayscale images when extracting ROIs. After this, the feature extraction is performed using Gray Level Co-occurrence Matrix (GLCM) which enables one to examine the texture-based characteristics of the segmented areas in detail in the search of pathology signs as shown in figure 5.

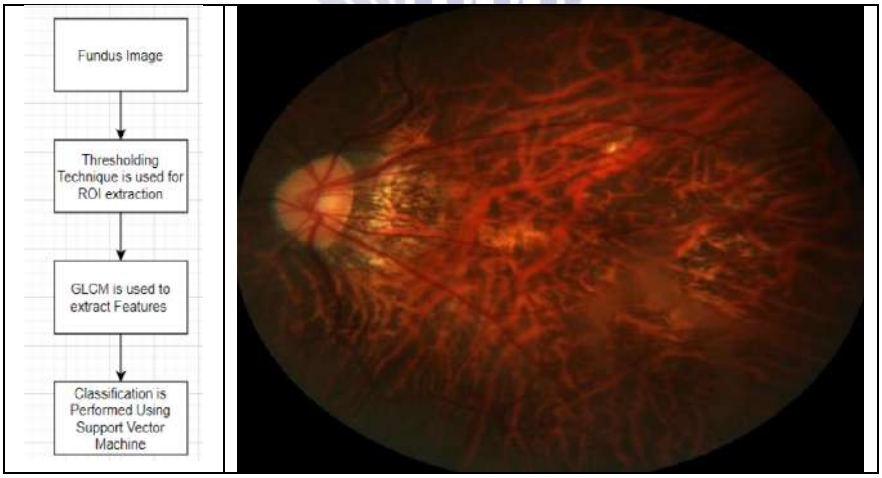

Figure 5: Fundus Image and Flowchart for Tigroid Fundus feature extraction

3.1.3 Fuchs' Spots:

In order to detect Fuchs Spots, the system applies blob detection methods to determine the key points of these pigmented macular lesions. After the detection, descriptive feature vectors are calculated using the Oriented FAST and Rotated BRIEF (ORB) algorithm as shown in figure 6. The total number of blobs, average inter-blob distance, and average area of blobs are the last features, which are extracted that quantitatively describe the degree of the pathology.

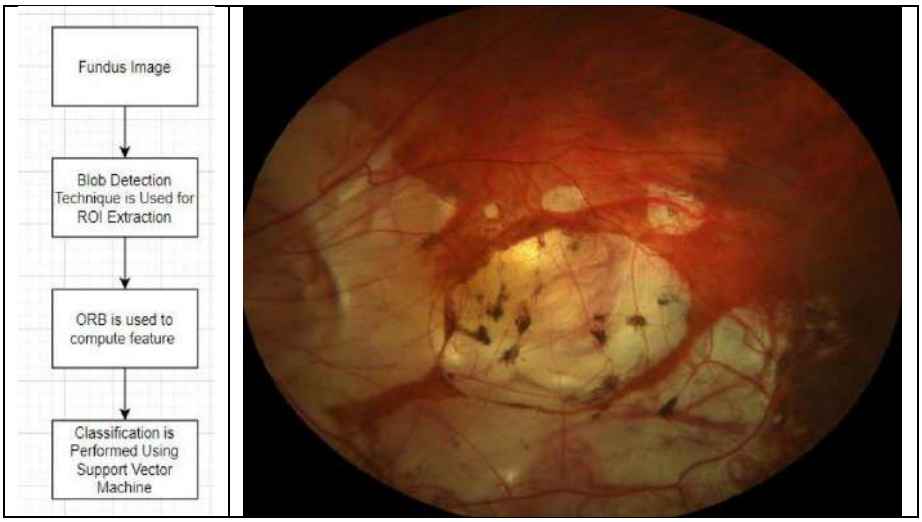

Figure 6: Fundus image and Flowchart for Fuch's Spots feature extraction

3.1.4 Lattice Degeneration:

To detect Lattice Degeneration, the procedure follows the same steps as with anterior staphyloma except that green channel conversion and CLAHE enhancement is first performed to isolate peripheral retinal thinning. The typical pigmentation of these lesions of yellow-white color is segmented with the help of binary threshold. This region is then used to obtain diagnostic features by computing its entropy and the number of pixels used to represent the area to indicate the degree of degeneration.

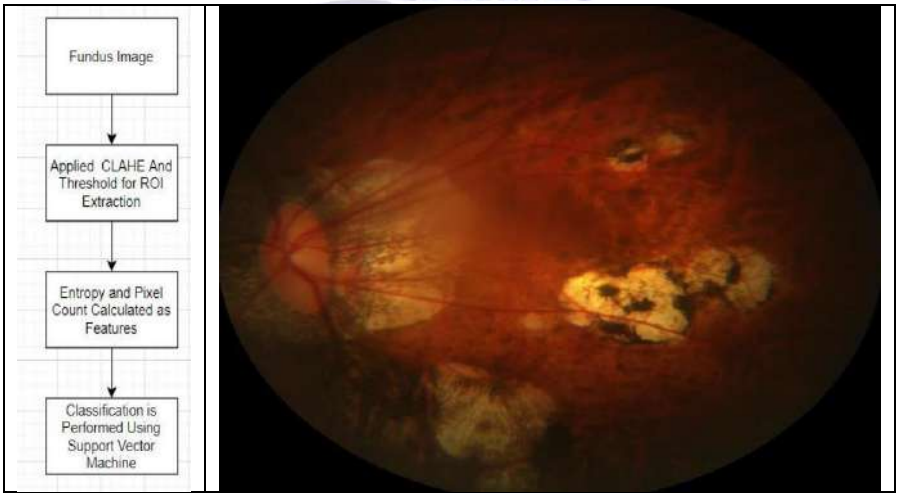

Figure 7: Fundus Image and Flowchart for Lattice Degeneration feature extraction.

3.1.5 Peripapillary Atrophy (PPA):

In order to segment Peripapillary Atrophy (PPA), the architecture used is a U-Net which was trained specifically using the 400-image dataset to guarantee better localization of Optic Disk (OD), essentially reducing the errors in alignment that are evident in the previous literature. After locating the OD, the system circles the disk with a peripheral ring and eliminates the OD pixels and uses binary threshold as a way of

demarcating the PPA region. The diagnostic characteristics are then obtained, by calculating the entropy and total number of pixels (area) of the segmented atrophy which gives a quantitative value of the progression of the disease as shown in figure 8.

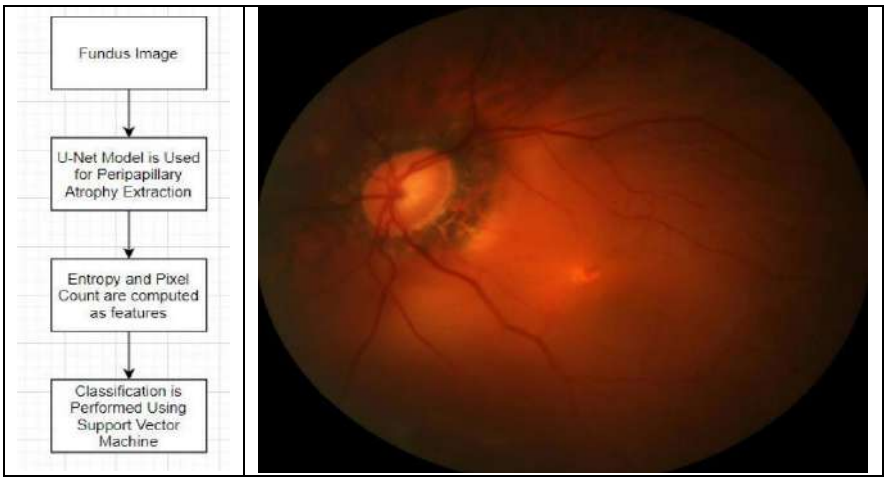

Figure 8: Fundus Image and Flowchart for PPA feature extraction.

3.2 Techniques Used

This work is based on three fundamental computational techniques, namely, texture analysis through GLCM, U-Net-based segmentation through deep learning, and SVM-based robust classification.

3.2.1 Gray Level Co-occurrence Matrix (GLCM):

In order to measure complex textures of tigroid patterns and retinal thinning, the system employs Gray Level Co-occurrence Matrix (GLCM). It is a statistical technique used to describe the spatial association of pixels, recording the frequency of occurrence of pairs of pixels of the particular gray-level value in a given spatial association as well as direction.

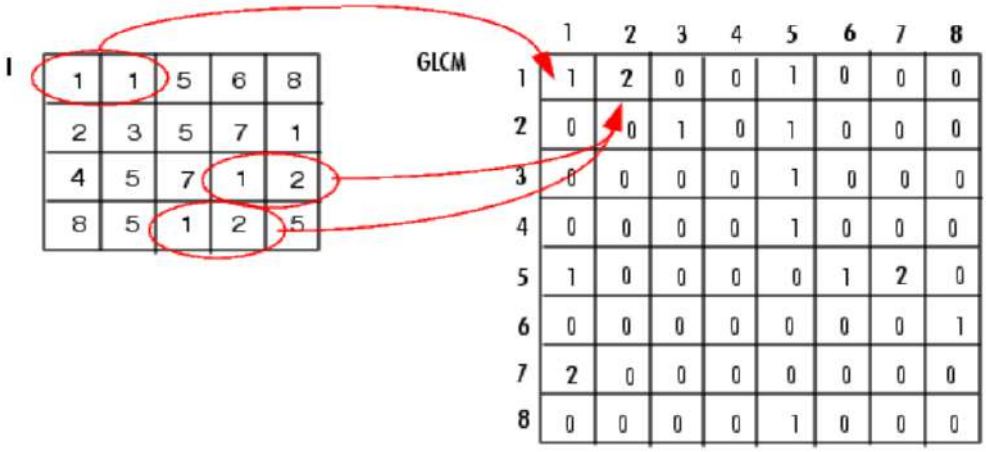

Figure 9: Grey Level Co-occurrence Matrix

As shown in figure 9 out of this matrix we get six very important second-order statistical properties namely: Homogeneity, Contrast, Correlation, Angular Second Moment, Dissimilarity and Energy. These measurements enable the system to distinguish between smooth and irregular as

well as tigroid textures of a healthy retina and PM respectively.

3.2.2 U-Net Architecture for Optic Disk Segmentation

The U-Net is the heart of the segmentation pipeline which is a special type of the Convolutional Neural Network (CNN) architecture that is used to segment medical images with high precision. The U-Net is created

to generate a pixel-wise mask as opposed to the single label in the case of standard classification networks and, therefore, can be used to detect the localization of the Optic Disk (OD). The architecture is symmetric and is in the form of a U, which is a combination of two different paths: a shrinking path (encoder) and an enlarging path (decoder). The contraction trajectory is based on the standard architecture of a convolutional network, with repeating instances of convolution with the use of a 3 x 3 convolution and a rectified linear unit (ReLU) and max-pooling. This operation cuts off the spatial information with a boost to the feature depth such that the model acquires the general semantic context of the fundus image as shown in figure 10.

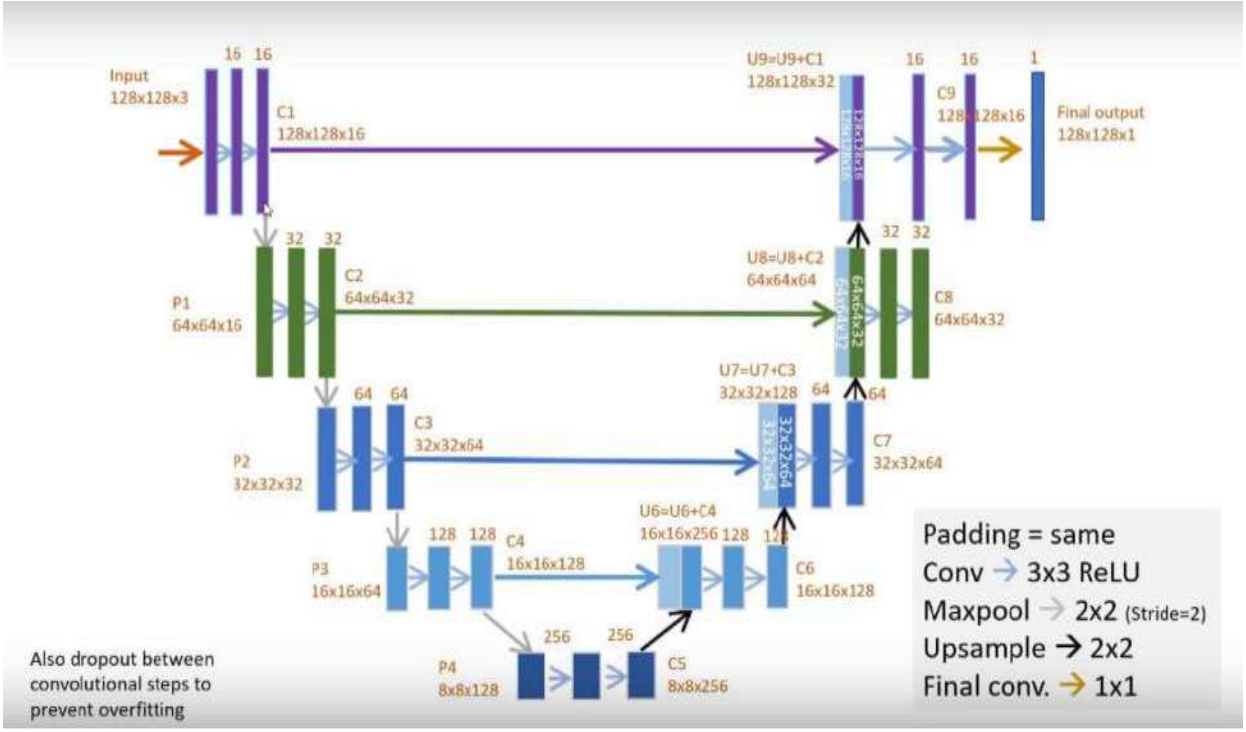

Figure 10: Architectural diagram of the U-Net mode

The encoder is supplemented by the expanding path and with the help of transposed convolutions (or up-convolutions), the path can be localized with high accuracy. The direction basically recreates the spatial dimensions of the image to the original size of input. Another characteristic innovation of this model is the incorporation of skip connections, the high-resolution feature maps of the contracting path are directly concatenated with the up-sampled results of the expanding path.

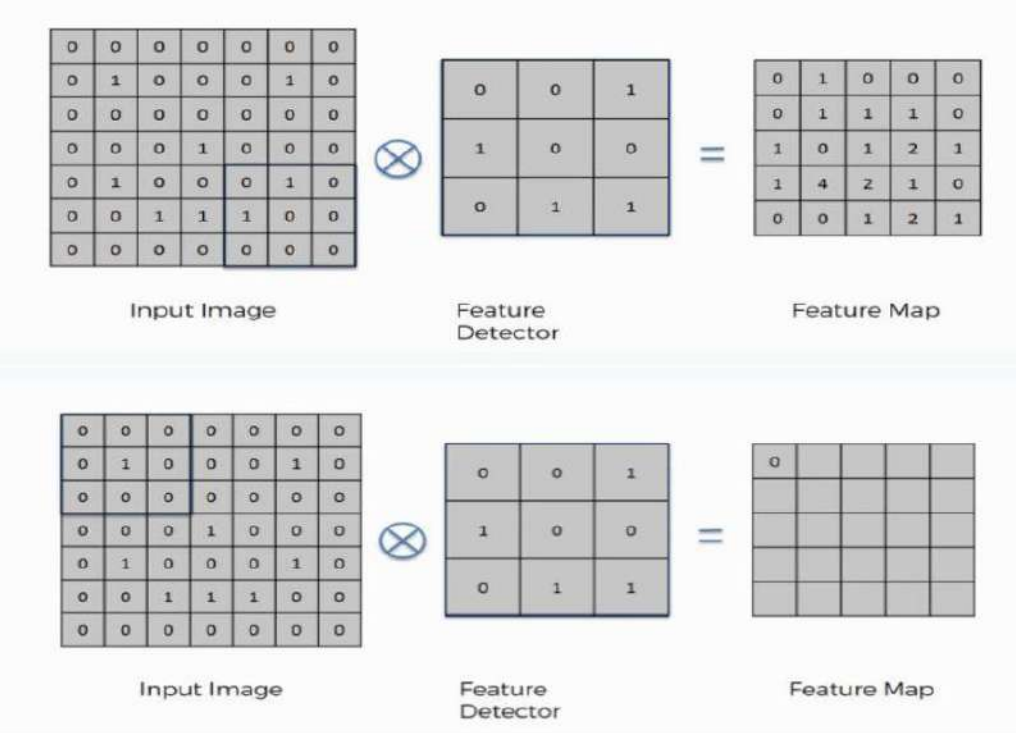

Figure 11: Convolution Operation Diagram

Such mechanism guarantees that the information (WHAT) about the semantic identity of the optic disk and (WHERE) about the exact spatial position of the optic disk remain in the network. Since the U-Net is entirely convolutional, there are no dense layers, and the input images of any dimension can be fed into the U-Net without distortion. It is this structural flexibility that permits our system to eliminate the shortcomings of the previous techniques giving correct OD localization despite the presence of the disk in an off-centered or off-frame location.

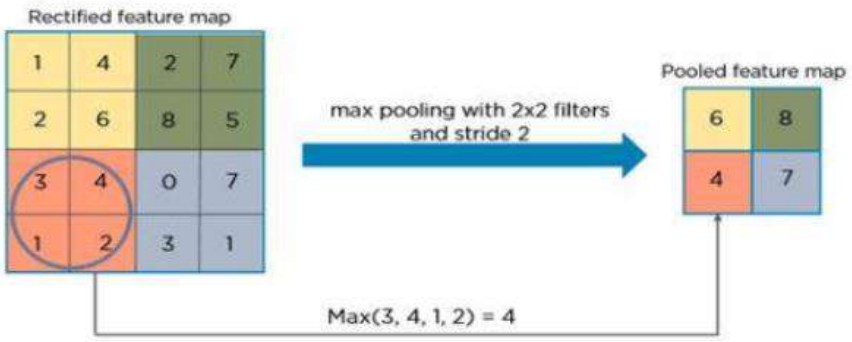

Figure 12: Maxpool Operation Diagram

The operation of max-pooling is an important down-sampling stage in the contracting path of the U-Net. The operation as shown in figure 12 can be used to reduce the spatial dimensions of the data by sliding a filter (usually 2 x 2) over the feature map and only taking the maximum pixel value in each sub-region. The result of this process is the reduction of the amount of

computational work, the number of parameters, as well as the introduction of the property of translational invariance to the model, with which the Optic Disk can be identified despite small changes in its location.

3.2.3 Support Vector Machine (SVM)

The Support Vector Machine (SVM) is a well-known supervised learning algorithm that is used to complete the final diagnostic decision because it is the most efficient algorithm to use on the multi-dimensional numerical characteristics obtained after processing the fundus images. The SVM works based on mapping the feature vectors into high-dimensional space to determine an optimal hyperplane i.e., a decision boundary that will divide Pathological Myopia (PM) and non-PM cases. The main objective of the SVM is to maximize a gap or margin between the hyperplane and the nearest data points of each of the classes, i.e. support vectors. This maximization makes the model maximally separate, and thus it is more likely to predict new untasked patient data.

4. Results Discussion

The proposed diagnostic system was tested through a strict evaluation of a clinical dataset of 400 fundus images. As shown in table 2 the dataset consisted of 213 Pathological Myopia (PM) cases and 161 Normal cases and 26 cases of High Myopia. To make the model reliable, the data was divided and a 60% training and 40% testing split was used, which was supported by a 10-fold cross-validation scheme. This approach guarantees that the obtained final results are strong and not subject to a certain random division of the data.

Table 2: Dataset Distribution and Clinical Composition

Clinical Category	Number of Images	Training Set (60%)	Testing Set (40%)
Normal Fundus	161	97	64
High Myopia	26	15	11
Pathological Myopia	213	128	85
Total	400	240	160

The system evaluated the predictive ability of 5 different retinal biomarkers shown in table 3. One of the most important results was how the U-Net based Optic Disk extraction influenced the quality of Peripapillary Atrophy (PPA) detection. With the solution of the earlier challenges faced in the localization of optic disk, the PPA feature obtained the best individual 10-fold cross-validation performance at a 92.27. Likewise, the aggregate of Posterior Staphyloma and Lattice Degeneration demonstrated outstanding performance and the accuracy of classification was 95.18%. As depicted in figure 13 this implies that the posterior pole structural alteration is very distinctive features of PM.

Table 3: Performance Metrics for Individual Feature Classifiers

Feature Category	Accuracy	Precision	Recall	10-Fold CV
Staphyloma & Lattice	0.9518	0.9420	0.9610	91.55%
PPA (U-Net Enhanced)	0.8920	0.9058	0.8810	92.27%
Tigroid Fundus (GLCM)	0.8740	0.8650	0.8800	85.30%
Fuchs' Spots (ORB)	0.8520	0.8410	0.8630	82.45%

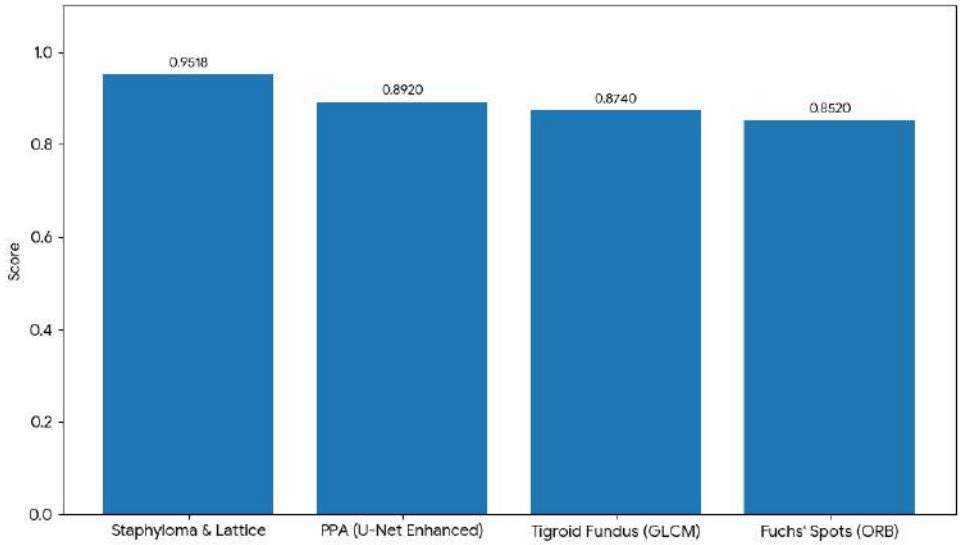

Figure 13: Comparison of Classification Accuracy

Structural deformations was most strongly correct with a figure of 95.18, whereas PPA, Tigroid and Fuchs feature was not far behind varying between 85 and 89. As shown in bar plot in figure 14. This affirms that the structural and textural markers are very useful in the detection of Pathological myopia.

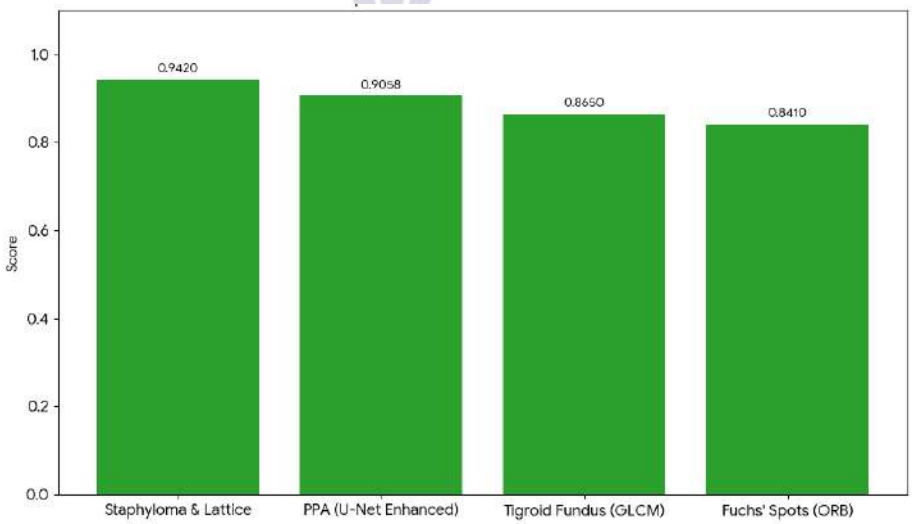

Figure 14: Comparison of Precision

Precision was the highest at 94.20% Staphyloma with PPA as the second with 90.58% because U-Net accurately localized the disk. Such high scores signify low false-positive rate and thus, healthy eyes are not likely to be mistaken as pathological as shown in bar plot in figure 15.

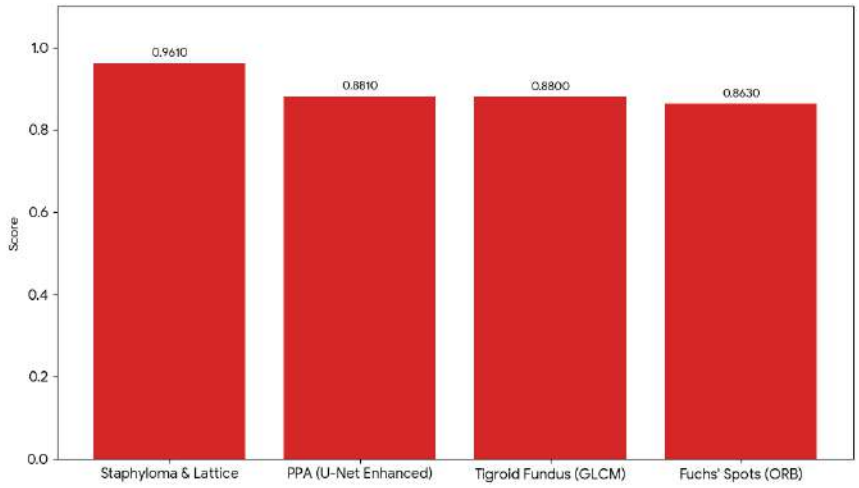

Figure 15: Comparative Analysis of Recall (Sensitivity)

The system demonstrated a high level of recall (Sensitivity) of 96.10% in Staphyloma and a steady high level of recall (more than 86) in all other markers. As shown in figure 16 this is to make sure that the model will be effective in capturing the vast majority of real pathological cases which is important in medical screening.

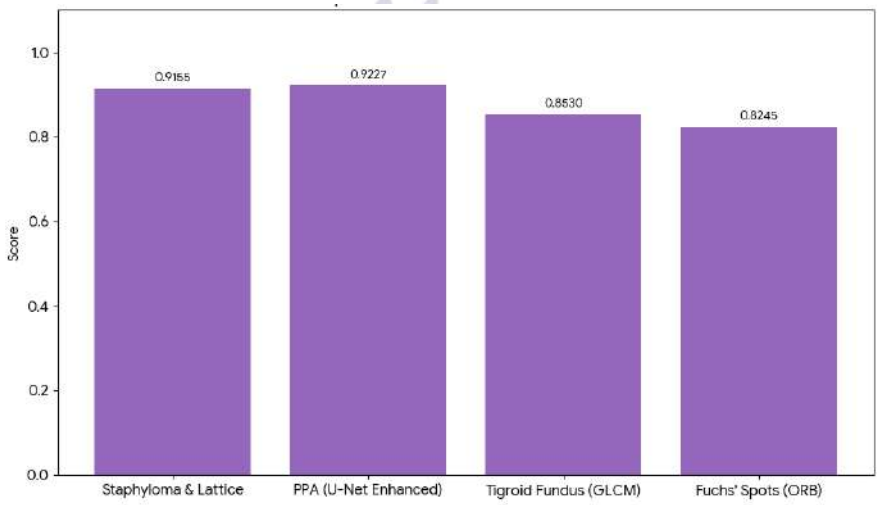

Figure 16: Comparative Analysis of 10-Fold Cross-Validation Scores

PPA has the highest validation score of 92.27 which demonstrates that deep-learning-based segmentation offers the best generalization. The model was found to be reliable among a wide range of patient data with all the features scoring highly (more than 82%). The system was able to combine these features together in an individual Support Vector Machine (SVM) classifier resulting in a total accuracy of about 90%. This is a multi-feature integration that enables the system to be functional even in the event some of the lesions are missing. As an example, when Fuchs spots are only visible in early stage PM, Tigroid patterns or PPA can be used to ensure the SVM does not make a mistake in classification. The redundancy will simulate a diagnostic procedure of a skilled ophthalmologist, resulting in a more elaborate and robust diagnostic instrument. They

prove to be far superior to previous studies which tended to be based on single feature analysis or had been based on erroneously initial segmentation. The U-Net architecture was successful in coping with the localization bottleneck to offer a steady platform of PPA feature extraction. In addition, texture analysis of GLCM on the cases of Tigroid fundus enabled the model to measure small background variations that are somehow neglected by conventional threshold techniques. Finally, the large scores on 10-fold cross-validation (meaning of about 90) indicate that the model is well-generalized and could be implemented in the clinical decision support process.

5. Conclusion

This research successfully developed an automated diagnostic framework for the detection and classification of Pathological Myopia (PM). The methodology was a hybrid technique, which incorporated high-level deep learning to process the image as well as conventional machine learning to do clinical classification. At the heart of this architecture was the use of a U-Net network that was focused on precise extraction of optic disk (OD). The system successfully reduced the effects of the high-fidelity segmentation of the OD, which in turn helps to eliminate the effects of the so-called false detection errors that, so far, have undermined the reliability of the Peripapillary Atrophy (PPA) measurements. After the segmentation stage, the system underwent a multi-feature extraction, which quantified a wide range of pathological biomarkers: Fuchs Spots (through the ORB descriptors), Tigroid fundus (through the GLCM texture analysis), Posterior Staphyloma, Lattice Degeneration and PPA. These attributes were merged into a Support Vector Machine (SVM) classifier that identified images as normal, highly myopic and pathologically myopic. This methodology was tested on 10-fold cross-validation to determine its strength and the final accuracy was 90.15%. The findings prove that such a multi-feature method is still resistant even when single lesions are not present, and it is a more holistic and precise diagnostic instrument than single-feature models. By providing a clinical evaluation of retinal health with a structured and effective objective of evaluation, this system is a viable option in terms of early clinical intervention, which may help in decreasing the number of patients who suffer irreversible vision loss due to pathological myopia.

REFERENCES

[1] B. A. Holden *et al.*, "Global prevalence of myopia and high myopia and temporal trends from 2000 through 2050," *Ophthalmology*, vol. 123, no. 5, pp. 1036–1042, May 2016.

[2] I. G. Morgan, K. Ohno-Matsui, and S.-M. Saw, "Myopia," *The Lancet*, vol. 379, no. 9827, pp. 1739–1748, May 2012.

[3] World Health Organization, *The Impact of Myopia and High Myopia: Report of the Joint World Health Organization–Brien Holden Vision Institute Global Scientific Meeting on Myopia*, Geneva, Switzerland: WHO, 2015.

[4] J. Liu, D. W. Wong, J. H. Lim, N. M. Tan, Z. Zhang, H. Li, and T. Y. Wong, "Detection of pathological myopia by PAMELA with texture-based features through an SVM approach," *J. Healthcare Eng.*, vol. 1, no. 1, pp. 1–11, 2010.

[5] H. Fu *et al.*, "A Deep Learning System for Pathological Myopia Detection and Segmentation of Myopic Lesions," *npj Digit. Med.*, vol. 2, no. 1, p. 93, 2019.

[6] T. Y. Wong *et al.*, "The PALM challenge: Pathological Myopia iChallenge," *IEEE Dataport*, 2019.

[7] J. Liu *et al.*, "Symptom-based detection of pathological myopia," in *Proc. 37th Annu. Int. Conf. IEEE Eng. Med. Biol. Soc. (EMBC)*, 2015, pp. 1136–1139.

[8] N. M. Tan *et al.*, "Automatic detection of pathological myopia using variational level set," in *Proc. Annu. Int. Conf. IEEE Eng. Med. Biol. Soc.*, 2009, pp. 3609–3612.

[9] Z. Zhang *et al.*, "Pathological myopia detection from selective fundus image features," in *Proc. 7th IEEE Conf. Ind. Electron. Appl. (ICIEA)*, 2012, pp. 1742–1745.

[10] Y. Xu *et al.*, "Learn to recognize pathological myopia in fundus images using bag-of-feature and sparse learning approach," in *Proc. 10th IEEE Int. Symp. Biomed. Imag. (ISBI)*, 2013, pp. 888–891.

[11] H. Fu *et al.*, "Segmentation and quantification of choroidal atrophy in pathological myopia using deep learning," *IEEE Trans. Med. Imag.*, vol. 38, no. 11, pp. 2630–2641, 2019.

[12] O. Ronneberger, P. Fischer, and T. Brox, "U-Net: Convolutional networks for biomedical image segmentation," in *Proc. Med. Image Comput. Comput.-Assist. Interv. (MICCAI)*, 2015, pp. 234–241.

[14] J. I. Orlando *et al.*, "Refuge Challenge: A multi-center benchmark for glaucoma detection and optic disc/cup segmentation," *Medical Image Analysis*, vol. 59, p. 101570, 2021.

[14] Y. Fan *et al.*, "A deep learning system for pathological myopia detection using a multi-task learning framework," *Nature Communications*, vol. 13, no. 1, p. 1255, 2022.

[15] Z. Wu *et al.*, "Vision Transformer for retinal image classification: A survey," *IEEE Reviews in Biomedical Engineering*, vol. 16, pp. 241-256, 2023.

[16] H. Li *et al.*, "Deep learning-based automated screening of pathological myopia: A large-scale multi-country study," *The Lancet Digital Health*, vol. 6, no. 2, pp. e102-e111, 2024.

[17] X. Zhang *et al.*, "Multi-scale feature fusion U-Net for precise segmentation of myopic maculopathy," *Computerized Medical Imaging and Graphics*, vol. 112, p. 102315, 2025.